

3D ANALYSIS OF MAGNETIC ANISOTROPIES IN OI AND CVI FILMS

S. SWAVING¹, G.J. GERRITSMAN, J.C. LODDER and Th.J.A. POPMA

Twente University, P.O. Box 217, 7500 AE Enschede, The Netherlands

Received 8 December 1986

In this paper a general model is presented to describe torque curves for a thin magnetic film with two anisotropy axes. One axis is assumed to lie in the plane of the film, having first-order anisotropy only, whereas the other one, having first- and second-order anisotropy, makes an arbitrary angle with the normal to the film. Given the parameters of the model, explicit expressions can be derived for both in-plane as well as perpendicular torque measurements with an infinite magnetic field. With some restrictions analytical expressions are derived to obtain the model parameters from the Fourier coefficients of experimentally obtained torque curves. Furthermore several methods are discussed to obtain finite-field corrections, including a power series expansion in the inverse magnetic field of the Fourier coefficients. An analytical expression was also derived to determine the direction of the easy axis. The applicability of the model is tested on a metal evaporated tape and we found it gave a consistent and quite accurate description of the torque curves of such a film. With this three-dimensional model the accuracy of the determination of the material parameters increases considerably, especially for the relatively weak transverse anisotropy of the film.

1. Introduction

Non-particulate coatings in the form of deposited metallic films are very promising aids in the development of magnetic recording media with increased storage capacity. In producing these Metal Evaporated (ME) tapes the principle of the so-called Oblique Incidence (OI) evaporation is applied. This method is modified in order to make it suitable for large scale production and a number of names for this modification have been suggested by various authors: e.g. the method of "High Incidence angle of Nucleation" (HIN) [1,2], "High Vacuum Electron Beam Roll Coating" [3] or "Continuously Varied Incidence" (CVI) [4-6]. The essential part of this method is the fact that metal atoms are evaporated and deposited on a substrate, while only a limited and continuously varying angle of incidence is permitted, therefore we prefer the name CVI method.

Both methods result in a columnar structure, with straight or curved columns for the OI and

CVI methods, respectively, and at least for OI films these columns are observed to be arranged in transversal bundles. These observations led to the introduction of two mutually perpendicular magnetic anisotropy axes, additional to the anisotropy because of the sheet demagnetization of the thin film, in order to be able to describe the anisotropic behaviour at high fields [7,8]. One anisotropy axis is directed along the columnar axis and the other along the transversal bundling direction.

Based on this model, a more general anisotropy model is presented here, which is expected to be very suitable for describing the results of torque measurements on both OI and CVI films, but also contains the simpler cases of films with longitudinal or perpendicular anisotropy.

In practical torque measurements the applied field is usually not strong enough (in our $H \leq 1600$ kA/m) to force the magnetization completely in the field direction. Therefore it is necessary to make a correction for the finite field, before fitting the measured curves to the model. We discuss some of the methods that are available for this purpose and present an analytical expression for

¹ Now at Philips Research Laboratories, P.O. Box 80000, 5600 JA Eindhoven, The Netherlands.

such a correction. However in the derivation of this expression, just as in all conventional methods, it is assumed that the magnetization will stay in the plane of the torque measurement (two-dimensional (2D) treatment). This is only true if the factual (three-dimensional (3D)) easy axis lies in this plane. If not, then it is quite conceivable that the magnetization vector will rotate out of the measurement plane, and will be slightly directed towards the easy axis.

In order to know the direction of the factual easy axis relative to the measurement plane we introduce here a 3D analysis of the direction of the easy axis as a function of direction and magnitude of the anisotropies. Furthermore we present 3D finite-field corrections for torque curves.

The results of our measurements and calculations show that a 3D interpretation of a torque curve can differ considerably from a 2D interpretation.

2. Description of the anisotropy model

In the model presented here, one anisotropy axis is assumed to be present in the longitudinal or incidence (yz -) plane (fig. 1), making an angle α with the film normal. The other anisotropy axis

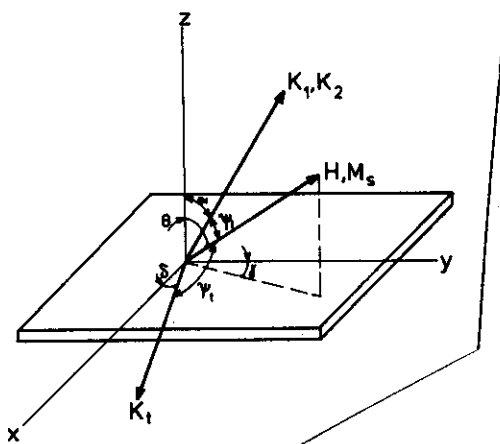


Fig. 1. Definition of axes with respect to film plane. The longitudinal yz -plane contains a uniaxial anisotropy axis, whereas the other axis lies in the film plane, making an angle δ with the transversal xz -plane.

is considered to lie in the film plane, making an angle δ with the transversal x -axis. The longitudinal anisotropy is characterized by first- and second-order anisotropy constants K_1 and K_2 , respectively, and the in-plane anisotropy (in the xy -plane) by one first-order constant K_1 . In addition to these two uniaxial anisotropy axes, the film plane acts as an anisotropy plane because of the sheet demagnetization of the thin film. Because of this 3D configuration of anisotropies it is insufficient to perform torque measurements in just one plane. Therefore in our model various measurement planes are considered. For reasons of simplicity concerning both the mathematics as well as the measurements themselves, it is obvious the only planes that are considered are either perpendicular to or parallel with the film plane.

2.1. Measurement plane perpendicular to the film plane

Torque measurements are assumed to be made in a plane that is perpendicular to the film plane and making an angle γ (fig. 1) with the longitudinal y -direction. In this way the situation of the three mixed uniaxial anisotropies is factually considered, resulting in a torque curve that corresponds to one single effective anisotropy in the measuring plane [9]. For the present it is assumed that the applied magnetic field is strong enough to keep the magnetization parallel to the field direction. If the field H and the magnetization M_s make an angle θ with the film normal, an angle ψ_1 with the in-plane anisotropy and an angle ψ_2 with the longitudinal anisotropy then the total anisotropy energy per unit volume becomes

$$E_a = K_1 \sin^2 \psi_1 + K_2 \sin^4 \psi_1 + K_1 \sin^2 \psi_2 + \frac{1}{2} \mu_0 M_s^2 \cos^2 \theta. \quad (1)$$

From the energy expression the torque L per unit volume can be derived

$$L = -dE_a/d\theta \quad (2)$$

and the result can be given in either rectangular or polar representations

$$L = \sum_{n=1}^2 (P_n \sin 2n\theta + Q_n \cos 2n\theta) \quad (3)$$

$$= \sum_{n=1}^2 L_n \sin 2n(\theta + \beta_n), \quad (4)$$

respectively, which are related by

$$L_n = \frac{P_n}{|P_n|} \sqrt{P_n^2 + Q_n^2}, \quad (5)$$

$$\tan(2n\beta_n) = Q_n/P_n. \quad (6)$$

Because of the straightforward interpretation of β_n ($-45^\circ < \beta_n < 45^\circ$), being the angle of the n th order easy axis with the film plane (if $L_n > 0$) or with the film normal (if $L_n < 0$), the polar representation can be very useful. With the substitutions

$$\cos \psi_1 = \sin \alpha \cos \gamma \sin \theta + \cos \alpha \cos \theta \quad (7)$$

and

$$\cos \psi_t = \sin(\gamma + \delta) \sin \theta \quad (8)$$

the following result for the amplitudes of the Fourier series of the torque can be derived

$$\begin{aligned} P_1 = & \frac{1}{2}\mu_0 M_s^2 - (K_1 + K_2) \cos 2\alpha \\ & - (K_1 + 2K_2) \sin^2 \alpha \sin^2 \gamma \\ & + K_2 \sin^4 \alpha (2 \sin^2 \gamma - \sin^4 \gamma) \\ & + K_1 \sin^2(\gamma + \delta), \end{aligned} \quad (9a)$$

$$Q_1 = [(K_1 + K_2) \sin 2\alpha + K_2 \sin^2 \alpha \sin 2\alpha \sin^2 \gamma] \times \cos \gamma, \quad (9b)$$

$$\begin{aligned} P_2 = & \frac{1}{2}K_2 [\cos 4\alpha + (\frac{3}{4} - \frac{3}{4}\cos 4\alpha - 2 \sin^4 \alpha) \sin^2 \gamma \\ & + \sin^4 \alpha \sin^4 \gamma], \end{aligned} \quad (9c)$$

$$Q_2 = -\frac{1}{2}K_2 [\sin 4\alpha + 2 \sin 2\alpha \sin^2 \alpha \sin^2 \gamma] \cos \gamma. \quad (9d)$$

Many of the most important special cases can be derived from these general expressions.

One special case of interest, to which we will limit ourselves in the theoretical considerations of the following sections, is that where the second-order anisotropy constant K_2 is negligible and the in-plane anisotropy axis lies along the transversal direction ($\delta = 0^\circ$) (i.e. the x -axis). This limitation is justified by the experimental results in section 6,

from which this appears to give a very realistic model of a CoNi CVI film.

With these assumptions it follows from a longitudinal measurement ($\gamma = 0^\circ$) that

$$L_1^2 = (\frac{1}{2}\mu_0 M_s^2 - K_1 \cos 2\alpha)^2 + (K_1 \sin 2\alpha)^2 \quad (10a)$$

$$\tan 2\beta_1 = K_1 \sin 2\alpha / (\frac{1}{2}\mu_0 M_s^2 - K_1 \cos 2\alpha) \quad (10b)$$

from which K_1 and α can be determined with

$$K_1^2 = (\frac{1}{2}\mu_0 M_s^2 - L_1 \cos 2\beta_1)^2 + (L_1 \sin 2\beta_1)^2 \quad (11a)$$

and

$$\tan 2\alpha = L_1 \sin 2\beta_1 / (\frac{1}{2}\mu_0 M_s^2 - L_1 \cos 2\beta_1). \quad (11b)$$

From an additional transversal measurement ($\gamma = 90^\circ$) K_t can also be determined

$$K_t = L_1 - \frac{1}{2}\mu_0 M_s^2 + K_1 \cos^2 \alpha. \quad (11c)$$

2.2. Film plane as measurement plane

Using the film plane as a measurement plane is particularly useful in determining whether $\delta = 0^\circ$ i.e. whether the in-plane anisotropy is directed along the transversal direction. Now $\theta = \pi/2$ and $L = -dE_a/d\gamma$ from which follows

$$P_1 = -(K_1 + 2K_2) \sin^2 \alpha + K_2 \sin^4 \alpha + K_1 \cos 2\delta, \quad (12a)$$

$$Q_1 = K_1 \sin 2\delta, \quad (12b)$$

$$P_2 = \frac{1}{2}K_2 \sin^4 \alpha, \quad (12c)$$

$$Q_2 = 0. \quad (12d)$$

It is clear that a zero phase shift of the torque curve ($\beta_1 = 0^\circ$) implies that δ is either 0° or 90° . If $L_1 > 0$ then $\delta = 0^\circ$, if $L_1 < 0$ additional measurements in other measuring planes are required to distinguish between the two possibilities.

The relative simplicity of equations (12a-d) stems from the fact that the torque in this specific measurement plane is independent of the sheet

demagnetization, so that in effect only two uniaxial anisotropies have to be taken into account.

3. Finite-field correction for torque curves

It is well known that in practical torque measurements it is almost impossible to apply high enough magnetic fields to make the field H and the magnetization M_s completely collinear. Therefore in the energy expression an extra field-energy term emerges, representing the potential energy of the magnetic moment in an external field

$$E = E_a + E_H \quad (13)$$

with

$$E_H = -\mu_0 H M_s \cos \psi_H \quad (14)$$

The angle ψ_H is the angle between the field direction and the direction of the magnetization. The direction of magnetization M_s is given by two angles (fig. 2): ϕ_1 is the angle between M_s and the film normal and ϕ_2 is the angle between the longitudinal axis and the plane defined by M_s and the film normal.

With $\delta = K_2 = 0$ the anisotropy-energy per unit volume is given by

$$E_a = \frac{1}{2} \mu_0 M_s^2 \cos^2 \phi_1 + K_1 \sin^2 \psi_1 + K_t \sin^2 \psi_t \quad (15)$$

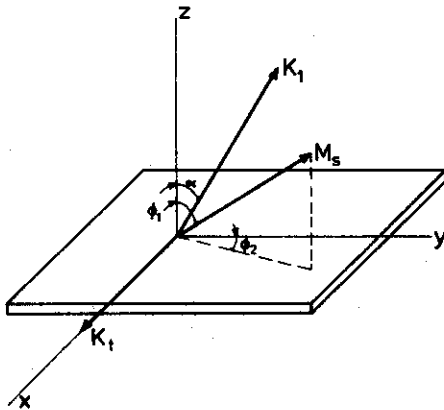


Fig. 2. Definition of axes for the 3D model, where M_s is allowed to rotate freely in three dimensions (angles ϕ_1 , ϕ_2) towards the directions of minimum energy.

with

$$\cos \psi_1 = \sin \alpha \cos \phi_2 \sin \phi_1 + \cos \alpha \cos \phi_1 \quad (16)$$

and

$$\cos \psi_t = \sin \phi_2 \sin \phi_1 \quad (17)$$

analogous to (1), (7) and (8). The angle-dependent part of the anisotropy energy can be written as

$$E_a = \frac{1}{2} B \sin^2 \phi_2 + \frac{1}{2} (A - B \sin^2 \phi_2) \cos 2\phi_1 - \frac{1}{2} C \cos \phi_2 \sin 2\phi_1 \quad (18)$$

with the definitions

$$A = \frac{1}{2} \mu_0 M_s^2 - K_1 \cos 2\alpha, \quad (19a)$$

$$B = K_1 \sin^2 \alpha - K_t, \quad (19b)$$

$$C = K_1 \sin 2\alpha. \quad (19c)$$

If the field direction is represented by the angle θ and γ as in fig. 1, then ψ_H is given by

$$\begin{aligned} \cos \psi_H = & \sin \phi_1 \sin \phi_2 \sin \theta \sin \gamma \\ & + \sin \phi_1 \cos \phi_2 \sin \theta \cos \gamma \\ & + \cos \phi_1 \cos \theta. \end{aligned} \quad (20)$$

Usually, in the 2D treatment, M_s is assumed to stay in the plane in which H rotates, i.e. $\phi_2 = \gamma$. Then (20) reduces to

$$\cos \psi_H = \cos(\phi_1 - \theta). \quad (21)$$

Now the contribution of the field energy makes it impossible to derive an explicit expression for the torque $L(\theta)$ as in section 2. If a torque measurement is performed in the longitudinal plane ($\gamma = \phi_2 = 0^\circ$) then minimization of the energy given by (13), (14), (18) and (21), yields

$$\begin{aligned} \partial E / \partial \phi_1 = & -(A \sin 2\phi_1 + C \cos 2\phi_1) \\ & + \mu_0 H M_s \sin(\phi_1 - \theta) = 0 \end{aligned} \quad (22)$$

or in polar representation

$$-L_1 \sin 2(\phi_1 + \beta) + \mu_0 H M_s \sin(\phi_1 - \theta) = 0 \quad (23)$$

with

$$L_1 = \frac{A}{|A|} \sqrt{A^2 + C^2} \quad (24a)$$

and

$$\tan 2\beta = C/A. \quad (24b)$$

The torque is given by

$$\begin{aligned} L(\theta) &= -\frac{dE}{d\theta} = -\frac{\partial E}{\partial \theta} - \frac{\partial E}{\partial \phi_1} \frac{\partial \phi_1}{\partial \theta} = -\frac{\partial E}{\partial \theta} \\ &= \mu_0 H M_s \sin(\phi_1 - \theta). \end{aligned} \quad (25)$$

Combining (23) and (25) yields an implicit expression for the torque in the longitudinal plane

$$\phi_1 = \theta + \arcsin(L(\theta)/\mu_0 H M_s), \quad (26a)$$

$$L(\theta) = L_1 \sin 2(\phi_1 + \beta). \quad (26b)$$

A number of methods are now available to solve these equations for a practical torque measurement.

If the measuring equipment offers the possibility of processing the experimental data, a general method is to first calculate ϕ_1 for every measuring point $(\theta, L(\theta))$ and then to expand the corrected torque curve into a Fourier series, from which the values of L_1 and β can be easily determined.

However, if the torque is not corrected before expanding into a Fourier series, then the Fourier coefficients themselves must be corrected. One possibility is to measure the coefficients as a function of the applied field H and to extrapolate to an infinite field, while another method makes use of approximate analytical corrections for the Fourier coefficients [10,11]. And finally a curve fitting procedure can be applied to fit the uncorrected measurement points straight away to the implicit function (26). The last two methods will be discussed in more detail.

3.1. Field dependence of the Fourier coefficients of the uncorrected torque curve

Dali et al. [10,11] use a first-order calculation to derive an expression for the field dependence of the Fourier coefficients. But more accurate corrections can easily be derived by presupposing a certain dependence of $\sin(\phi_1 - \theta)$ on $1/H$

$$\sin(\phi_1 - \theta) = s_1 \epsilon + s_2 \epsilon^2 + s_3 \epsilon^3 + \dots \quad (27)$$

with the definition

$$\epsilon = L_1/\mu_0 H M_s. \quad (28)$$

After substitution in the equilibrium expression (23) and up to order ϵ^5 the coefficients s_i of the expansion (27) can be deduced from

$$\begin{aligned} \epsilon \sin 2(\theta + \beta) &= \sin(\phi_1 - \theta) \{1 + 2\epsilon(\sin 2(\theta + \beta) \sin(\phi_1 - \theta) \\ &\quad - \cos 2(\theta + \beta)[1 - \frac{1}{2}\sin^2(\phi_1 - \theta)])\} \end{aligned} \quad (29)$$

so it follows for the expression of the torque (25) in powers of ϵ (up to the fourth order and the second harmonic) that

$$\begin{aligned} L(\theta) &= L_1 \{ (1 - \frac{1}{2}\epsilon^2 + 0\epsilon^4 + \dots) \sin 2(\theta + \beta) \\ &\quad + (\epsilon - \frac{3}{4}\epsilon^3 + \dots) \sin 4(\theta + \beta) \\ &\quad + (\frac{3}{2}\epsilon^2 - 3\epsilon^4 + \dots) \sin 6(\theta + \beta) \} \\ &= \sum R_n \sin 2n(\theta + \beta). \end{aligned} \quad (30)$$

Here R_n are the field-dependent Fourier coefficients of the uncorrected torque curve.

$$\lim_{H \rightarrow \infty} R_n = L_n. \quad (31)$$

It is noteworthy that the phase angles β are equal for all harmonics and do not show any field dependence. Furthermore an important implication from (30) is the fact that at high fields R_1 and R_3 are proportional to $1/H^2$ instead of $1/H$ as is R_2 . If L_1 is determined by extrapolation to infinite field, this should be taken into account.

Eq. (30) was derived for a torque measurement in the longitudinal plane but also holds for torque measurements performed in other planes, like the transversal and film planes. Only eq. (24) has to be adjusted for these cases; in the case of the transversal plane it follows from (9) and (19) that

$$L_1 = A - B \quad \text{and} \quad \beta = 0^\circ \quad (32)$$

and for the film plane it follows from (12) and (19) that

$$L_1 = -B \quad \text{and} \quad \beta = 0^\circ \quad (33)$$

It is important to realize that in the deduction of (30) it is assumed that M_s will always stay in the measurement plane. But if the 3D easy axis does not lie in this plane it is quite conceivable that the M_s -vector will rotate out of it. In the next section more attention will be paid to this problem.

3.2. Curve fitting of experimental torque curves

It may be helpful, to make use of a curve-fitting method, instead of using corrections and Fourier expansions, in order to determine the anisotropy parameters of the film. There are so many parameters (K_1 , K_2 , K_t , α , δ) and possibly also an offset in the torque because of rotational hysteresis losses L_0 and an offset in the angle because of incorrect mounting of the sample on the holder θ_0 , that is is very hard to find the optimum set of values that fits the experimental data best, if no curve-fitting procedure is used. If a zero finding procedure is included, the function that has to be fitted to the torque curve may have an implicit form as in (26), so that is is not necessary to make use of any corrections before fitting. Another advantage is the fact that only one torque measurement is sufficient in every measurement plane, preferably at an external magnetic field that is as high as possible.

The well-known Simplex algorithm is very suitable for a curve-fitting program.

4. 3D analysis of the easy direction

It is clear from the discussion in section 2, that in every measurement plane an easy direction is present where the energy is minimum, i.e. the torque is zero and has a negative slope. But this easy direction in the plane under consideration does not necessarily coincide with the factual 3D easy axis. This can be illustrated by a 3D analysis of the direction of minimum energy for the magnetization.

Consider the situation where no magnetic field is present and the direction of magnetization M_s is given by two angles ϕ_1 and ϕ_2 (fig. 2). The anisotropy energy as a function of the magnetization direction $E_a(\phi_1, \phi_2)$ has stationary points if

$$\partial E_a / \partial \phi_1 = \partial E_a / \partial \phi_2 = 0. \quad (34)$$

These stationary points represent an energy minimum if

$$\left(\frac{\partial^2 E_a}{\partial \phi_1^2} \right) \left(\frac{\partial^2 E_a}{\partial \phi_2^2} \right) - \left(\frac{\partial^2 E_a}{\partial \phi_1 \partial \phi_2} \right)^2 > 0 \quad (35a)$$

and

$$\left(\partial^2 E_a / \partial \phi_1^2 \right) > 0. \quad (35b)$$

Introducing two dimensionless parameters namely

$$A' = A / |C| \quad (36a)$$

and

$$B' = 2B / |C| \quad (36b)$$

it can be shown that the 3D easy axis has a direction along the transversal axis ($\phi_1 = \phi_2 = 90^\circ$) if $B' < A' - \sqrt{(A')^2 + 1}$ or somewhere in the longitudinal plane ($\phi_2 = 0^\circ$) if $B' > A' - \sqrt{(A')^2 + 1}$. In the latter case the angle ϕ_1 follows from

$$\cot 2\phi_1 = \pm A', \quad (37)$$

where the permitted ranges for ϕ_1 follow from the signs of A and C according to table 1.

For $C > 0$ the easy axis rotates from $\phi_1 = 0^\circ$ for $A' = -\infty$ to $\phi_1 = 90^\circ$ for $A' = +\infty$, whereas for $C < 0$ it rotates from $\phi_1 = 180^\circ$ to $\phi_1 = 90^\circ$. The former case is presented in fig. 3, where the bold lines separate three different regions. It is easy to show that the easy axis always has a direction in the longitudinal plane if $K_1 > \frac{1}{2}\mu_0 M_s^2$ and $K_t < K_1 - \frac{1}{2}\mu_0 M_s^2$.

In the limiting case $C = 0$, that is if $\alpha = 0^\circ$ or $\alpha = 90^\circ$, the easy axis no longer rotates in the easy plane, but assumes the limiting values $\phi_1 = 0^\circ$ for $A < 0$ and $\phi_1 = 90^\circ$ for $A > 0$. Furthermore the condition $B > 0$ for $A > 0$ and $B > A$ for $A < 0$ has to be fulfilled, otherwise the easy axis is directed along the transversal axis.

A very interesting comparison is that between the direction of the 3D and the 2D easy axes. As seen from (12a), the easy axis in the film plane

Table 1
Range of ϕ_1 as a function of the sign of the parameters A and C

A	C	ϕ_1 (degrees)
+	+	45-90
+	-	90-135
-	+	0-45
-	-	135-180

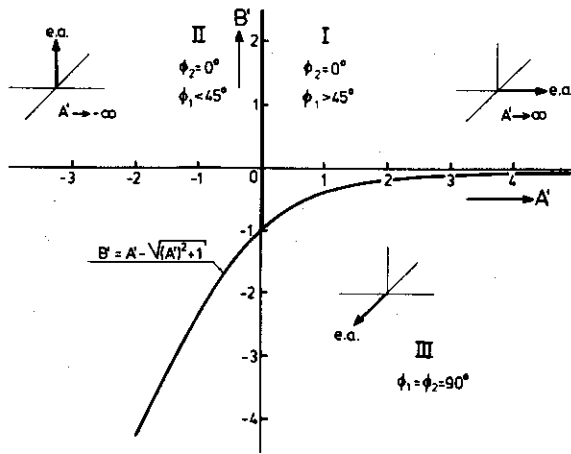


Fig. 3. Position of the easy axis in the 3D model. The parameter space $A'B'$ is divided into three regions. In region I $\phi_2 = 0^\circ$ and $45^\circ < \phi_1 \leq 90^\circ$. In region II $\phi_2 = 0^\circ$ and $0^\circ \leq \phi_1 < 45^\circ$. In region III $\phi_1 = \phi_2 = 90^\circ$. The thick solid lines separate the three regions.

will rotate from the transversal axis towards the longitudinal axis if $K_1 \sin^2 \alpha > K_t$, i.e. $B' > 0$. However, it can be concluded from fig. 3 that the "real" 3D easy axis already rotates from the transversal axis towards the longitudinal plane at a smaller value of B' viz. if $B' > A' - \sqrt{(A')^2 + 1}$. This can be understood by realizing that the assumption of M_s being confined to the film plane actually implies an infinite sheet demagnetization and thus an infinite high value of A' . And for A' approaching infinity the separation line between ranges I and III in fig. 3 approaches the line $B' = 0$, while at the same time the easy axis in the longitudinal plane approaches the longitudinal axis.

5. 3D finite-field correction for torque curves

With fig. 3 in mind it is simple to determine the easy direction of a certain film, once one has an approximate knowledge of the direction and magnitude of the anisotropies from a first rough 2D interpretation. Knowing this direction it is possible to determine the anisotropies more accurately by taking into account the direction of the easy

axis relative to the measurement plane.

For OI and CVI films evaporated at high incidence angles B' is usually positive, which means that the easy axis lies in the longitudinal plane. Therefore it is expected that for torque measurements performed in the longitudinal plane the 2D and 3D analyses will give identical results, but that for measurements in the transversal and film planes deviations will occur. In the 3D treatment the magnetization vector is allowed to rotate freely in three dimensions towards the direction of minimum energy. From the expression for the total free energy, given by (13), (14) and (18), the torque for arbitrary γ is given by

$$L(\theta) = -dE/d\theta \\ = \mu_0 H M_s [\sin \phi_1 \cos \theta \cos(\phi_2 - \gamma) - \cos \phi_1 \sin \theta], \quad (38a)$$

where ϕ_1 and ϕ_2 can be found from

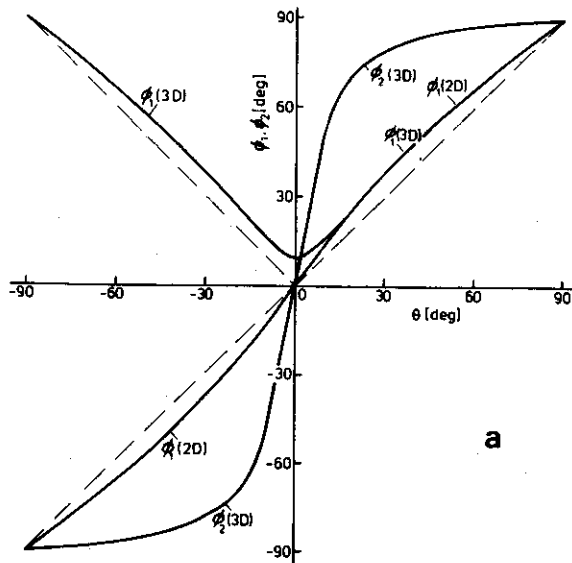
$$-\mu_0 H M_s \sin \theta \sin(\phi_2 - \gamma) \\ = B \sin 2\phi_2 \sin \phi_1 + C \sin \phi_2 \cos \phi_1, \quad (38b) \\ -\mu_0 H M_s [\cos \phi_1 \sin \theta \cos(\phi_2 - \gamma) - \sin \phi_1 \cos \theta] \\ = (A - B \sin^2 \phi_2) \sin 2\phi_1 + C \cos \phi_2 \cos 2\phi_1. \quad (38c)$$

For large values of the magnetic field it follows from eq. (38b) that $\phi_2 \approx \gamma$ and from eq. (38c) that $\phi_1 \approx \theta$ and the torque at high magnetic field is given by

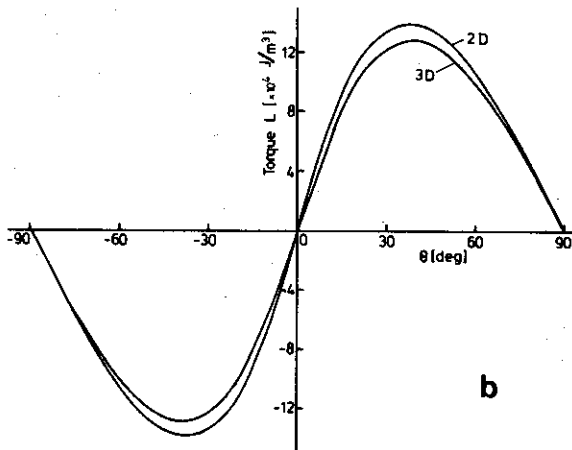
$$L(\theta) \approx (A - B \sin^2 \gamma) \sin 2\theta + C \cos \gamma \cos 2\theta \quad (39)$$

and the 2D case is regained. In order to illustrate the differences between the 2D and 3D cases for the transversal plane ($\gamma = 90^\circ$) the values of ϕ_1 and ϕ_2 are shown in fig. 4a as a function of the direction of the applied magnetic field. For some specific values of A , B , C , M_s and H . It is noticeable that the direction of M_s is not exactly in between the directions of the field and the 3D easy axis.

In fig. 4b the differences in the resulting torque are shown; which in the case of these specific parameters the amplitude as calculated with the realistic 3D analysis is more than 10% smaller



a



b

Fig. 4. (a) The rotation of the magnetization M_s during a transversal torque measurement, where θ = angle between magnetic field and the normal to the film. Both ϕ_1 and ϕ_2 are given for the 2D ($\phi_2 = 0^\circ$) and the 3D approach. The parameter values are $A = 18 \times 10^4 \text{ J/m}^3$, $B = 4 \times 10^4 \text{ J/m}^3$, $C = 12 \times 10^4 \text{ J/m}^3$ and $\mu_0 H M_s = 102 \text{ J/m}^3$. This results in an easy axis direction given by $\phi_1 = 73.2^\circ$ and $\phi_2 = 0^\circ$; (b) The calculated transversal torque for the 2D and the 3D approaches, where θ = angle between magnetic field and the normal to the film. The parameters are the same as with fig. 4a.

than the 2D amplitude. It is obvious that such a considerable difference will clearly affect the values of the anisotropy parameters as determined from experimental torque curves.

The implicit 3D function for torque measurements in the film plane can be derived in a completely analogous manner.

$$(A - B \sin^2 \phi_2) \sin 2\phi_1 + C \cos \phi_2 \cos 2\phi_1 + \mu_0 H M_s \cos(\phi_2 - \theta) \cos \phi_1 = 0, \quad (39a)$$

$$B \sin \phi_1 \sin 2\phi_2 + C \cos \phi_1 \sin \phi_2 + \mu_0 H M_s \sin(\phi_2 - \theta) = 0, \quad (39b)$$

$$L(\theta) = -B \sin^2 \phi_1 \sin 2\phi_2 - \frac{1}{2} C \sin 2\phi_1 \sin \phi_2. \quad (39c)$$

These can be compared with the 2D result from equations (26) and (33). For the same parameters as used in fig. 4b this results in a 3D amplitude of the torque curve, that is about 15% higher than the 2D amplitude.

Finally if the 3D analysis is applied to the longitudinal torque measurement, with these specific anisotropy parameters, then for every angle θ , we find $\phi_2 = 0^\circ$. This means that, just as expected, the 2D and 3D cases are equivalent if the 3D easy axis lies in the plane of the torque measurement.

6. Experimental torque measurements on a CVI film

Experimental evidence for the suitability of the theories as developed above is given by the results of the analysis of the anisotropic, magnetic behaviour of a CoNi CVI film. The saturation magnetization M_s of this film as determined with a VSM is about 510 kA/m, so that $\frac{1}{2} \mu_0 M_s^2 \approx 16.4 \times 10^4 \text{ J/m}^3$.

First we shall illustrate the use of the approximate analytical corrections of the Fourier coefficients of a longitudinal torque measurement and compare these with the result that can be derived with the method of Dali et al. [10,11].

Further as an illustration of the curve fitting method and the application of a 3D treatment, we shall describe the process of anisotropy parameter extraction of the CVI tape.

6.1. Analytical correction of the longitudinal torque curve

Torque measurements in the longitudinal plane are performed at six different field strengths between 800 and 1600 kA/m, while the angle θ is varied from -90° to $+90^\circ$. Eighteen measurement points are used from these torque curves to calculate the first, second- and third-order Fourier coefficients as functions of the field. As predicted in section 3.1 the phase angles do not show any dependence on the field or on the order of the harmonic.

In fig. 5 the field dependence of the Fourier coefficients of the uncorrected torque curves is shown. In accordance with eq. (30) R_1 and R_3 are plotted as a function of $(1/H)^2$ and R_2 as a function of $(1/H)$. Extrapolation of the curves to $(1/H) = 0$ suggests that L_2 and L_3 are negligible compared with L_1 , which justifies the use of eq.

(30). This equation provides the possibility to calculate the corrected values of the Fourier coefficients for every measurement point. For the first-order coefficient this is simply achieved by solving L_1 from

$$L_1 - \frac{1}{2} \frac{L_1^3}{(\mu_0 M_s)^2} \left(\frac{1}{H} \right)^2 - R_1 = 0, \quad (40)$$

the results of which are shown in fig. 5 together with those determined by the method of Dali et al. [10,11].

It is clear that the approximations of L_1 calculated with (40) are convincingly better, although some field dependence is still present. In other measurement planes this method is less satisfactory, but this is principally inherent in the 2D approach.

6.2. 3D determination of the anisotropy parameters

For the parameter extraction three torque curves are sufficient, measured at the highest achievable field in the longitudinal, transversal and film planes (1600, 1600 and 1440 kA/m, respectively). From each curve we used eighteen values of $(\theta, L(\theta))$ to perform a Simplex curve-fitting procedure.

It appeared to be essential to include two extra parameters θ_0 and L_0 , in order to account for offsets in the angle and the torque, respectively. Values for θ_0 never exceeded 2° , which is a realistic estimation of the deviation caused by inaccurate mounting of the sample. Values of L_0 were also always negative, which points to energy dissipation in the film during the rotation; i.e. the so-called rotational hysteresis loss.

The procedure to find the values for the model parameters was as follows: It appeared from a first rough 2D fit of the film plane curve, where temporarily K_2 was taken to be negligible, that the in-plane anisotropy K_1 was directed along the transversal axis, i.e. $\delta = 0^\circ$. A longitudinal fit with $\delta = 0^\circ$, then confirmed that the assumption of a small K_2 was justified. The value of K_2 was about 3% of the value of K_1 , so that K_2 was also set to zero. Another longitudinal fit with both $\delta = 0^\circ$ and $K_2 = 0$ provided the definite values of

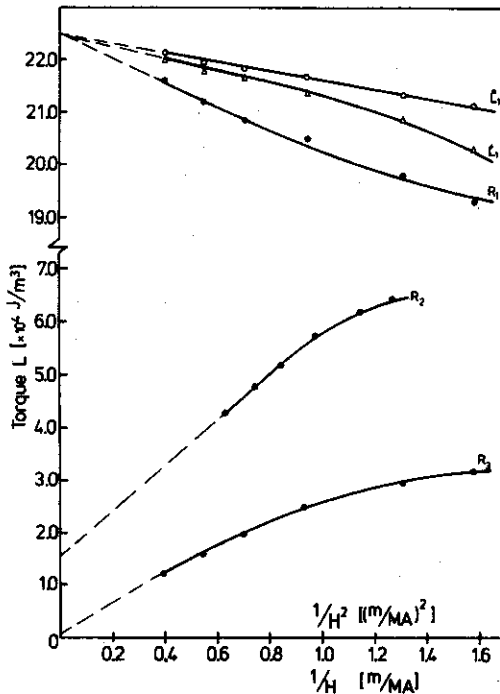


Fig. 5. The experimental Fourier coefficients R_1 , R_2 and R_3 versus $1/H^2$, $1/H$ and $1/H^2$, respectively. L_1' gives the Dali correction and L_1'' our correction for the first-order coefficient R_1 . The infinite field value $L_1 = 22.5 \times 10^4 \text{ J/m}^3$.

$K_1 = 12.3 \times 10^4 \text{ J/m}^3$ and $\alpha = 49.7^\circ$, so that K_t was the only parameter still unknown.

K_t could be determined from both the transversal and film plane torque data, with either the 2D or the 3D model. A relatively large discrepancy in K_t values was found for both models, because in first order K_t is the result of the subtraction of two, almost equal, large numbers (viz. $\frac{1}{2}\mu_0 M_s^2$ and $K_1 \cos^2\alpha$). However, by applying the 3D model this discrepancy could be reduced by a factor two, as is illustrated by the accuracy of the mean value for the 2D approach $K_t = (2.6 \pm 0.7) \times 10^4 \text{ J/m}^3$ and the 3D approach $K_t = (3.4 \pm 0.4) \times 10^4 \text{ J/m}^3$. Furthermore the 3D value is about 30% higher than the 2D value.

7. Conclusions

An important improvement has been presented on the existing anisotropy models for OI and CVI films by deriving explicit expressions for the torque in arbitrary measurement planes, by extending the concept of easy axis to three dimensions and by demonstrating the influence of three-dimensional rotation of the magnetization vector on finite field corrections for torque curves. Application to torque measurements of a CVI film provided a

very satisfactory description of the anisotropic behaviour at high fields. Of course it should be borne in mind, that these results are based on the concept of coherent rotation, of which the applicability is limited to high magnetic fields and homogeneous films.

References

- [1] K. Nakamura, Y. Ohta, A. Itoh et al., IEEE Trans. Magn. MAG-18 (1982) 1077.
- [2] Y. Ohta, K. Nakamura, A. Itoh et al., IEEE Trans. Magn. MAG-18 (1982) 1209.
- [3] A. Feuerstein and M. Mayr, IEEE Trans. Magn. MAG-20 (1984) 51.
- [4] Y. Iijima and K. Shinohara, National Technique Report 25 (1979) 1064 (in Japanese).
- [5] T. Kunieda, K. Shinohara and A. Tomago, The Fifth Intern. Conf. on Video and Data Recording, Southampton, England (1984).
- [6] K. Shinohara, H. Yoshida, M. Odagiri et al., IEEE Trans. Magn. MAG-20 (1984) 824.
- [7] K. Hara, T. Hashimoto and E. Tatsumoto, J. Phys. Soc. Japan 28 (1970) 254.
- [8] K. Hara, J. Sci. Hiroshima Ser. AII 34 (1970) 139.
- [9] M. Tejedor, M. Torres and B. Hernando, J. Magn. Magn. Mat. 42 (1984) 59.
- [10] Z. Dali, Z. Hui and C. Liya, J. Magn. Magn. Mat. 19 (1980) 412.
- [11] Z. Dali, Z. Hui, Z. Chuanli et al., J. Magn. Magn. Mat. 19 (1980) 415.